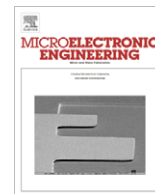




Contents lists available at ScienceDirect

Microelectronic Engineering

journal homepage: www.elsevier.com/locate/mee

SAW device integrated with microfluidics for array-type biosensing

K. Mitsakakis^{a,b}, A. Tserepi^d, E. Gizeli^{a,c,*}^a Institute of Molecular Biology and Biotechnology, Foundation for Research and Technology Hellas, Vassilika Vouton, GR-711 10 Heraklion, Greece^b Department of Materials Science and Technology, GR-710 03, University of Crete, Vassilika Vouton, Heraklion, Greece^c Department of Biology, University of Crete, GR-714 09 Vassilika Vouton, Heraklion, Greece^d Institute of Microelectronics, NCSR "Demokritos", P.O. Box 62230, GR-153 10 Athens, Greece

ARTICLE INFO

Article history:

Received 30 September 2008

Received in revised form 19 December 2008

Accepted 19 December 2008

Available online xxx

Keywords:

Biosensor

Microfluidics

Poly(dimethylsiloxane) (PDMS)

Surface acoustic waves (SAW)

ABSTRACT

This work describes the utilization of a multi-channel microfluidic module on a Surface Acoustic Wave (SAW) sensor chip in order to achieve multi-analyte detection. The design and fabrication issues of the microfluidics-on-SAW ("μF-on-SAW") setup are presented as well as the evaluation of the sensitivity of the system during glycerol and protein loading. In its current configuration, μF-on-SAW can host up to eight different analytes for detection on the dual-device chip, crossed by four parallel microchannels.

© 2009 Elsevier B.V. All rights reserved.

1. Introduction

Piezoelectric devices such as Quartz Crystal Microbalance (QCM) and Surface Acoustic Wave (SAW) devices have been successfully used for biosensing purposes, exhibiting high sensitivity in mass deposition [1], viscous and/or viscoelastic changes [2–4], as well as in the detection of conformational changes of surface-bound biomolecules [5,6]. In the majority of the applications, the operation of SAW and QCM sensors has followed the "one-sample-per-sensor" regime, detecting in real time one analyte (or, in general, one process) per device. However, recent advances in biology, e.g. in proteomics and genomics, as well as in medical diagnostics, require the development of platforms that are capable of detecting a large number of analytes leading to multiplexing of the results and better understanding of biomolecular interactions. So far, acoustic devices for multi-analysis make use of a linear array of M sensor elements [7,8] able to detect M liquid samples. Recently a novel approach has been described showing that the surface of a single SAW device can be compartmentalized into N sub-areas by using an N -channel microfluidic module made of poly(dimethyl siloxane) (PDMS) [9]. In the current work, this concept is expanded by using a dual SAW chip (i.e. $M = 2$ elements on the chip) in combination with a four-channel microfluidic module

for the multiple detection of aqueous solutions and protein samples on an array of 4×2 detection sub-areas.

2. Platform design and fabrication

The setup consists of a chip with two sensor elements and a four-channel microfluidic module [9]. The microfluidics are designed in a parallel channel format and cross the dual-sensor chip perpendicularly. Thus, an array of eight sub-areas is formed, on which eight distinct and independent experiments can be carried out.

2.1. SAW sensor chip

Sensor description: The main parts of a SAW (bio)sensor are the following (Fig. 1): (i) the piezoelectric substrate (quartz in our case), which supports the acoustic wave; (ii) the two sets of InterDigital Transducers (IDTs), which serve as the input and output of the electric signal. They are made of Au and are photolithographically patterned on quartz, with a Cr intermediate layer for adhesion purposes. The periodicity of the IDT fingers defines the wavelength (32 μm, operating frequency 155 MHz). (iii) On top of the IDTs, a thin polymer layer (polymethyl methacrylate, PMMA, few hundreds of nm thick) is spin-coated and acts as waveguide, supporting a Love wave [10]. For the experiments with proteins and for adsorption purposes, an additional 20 nm Au layer was sputter-coated on top of the PMMA and between the two IDT sets (not shown in Fig. 1).

Detection mechanism: Due to the piezoelectric nature of the substrate, the AC electrical input is transformed into a mechanical

* Corresponding author. Address: Institute of Molecular Biology and Biotechnology, Foundation for Research and Technology Hellas, Vassilika Vouton, GR-711 10 Heraklion, Greece. Tel.: +30 2810 304373; fax: +30 2810 394408.

E-mail address: gizeli@imbb.forth.gr (E. Gizeli).

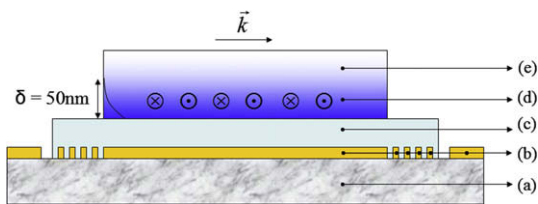


Fig. 1. Schematic side view of a SAW sensor. (a) piezoelectric substrate (quartz), (b) Au contact pads, IDTs and metallization area, (c) PMMA waveguide, (d) shear-horizontal polarization of the wave, (e) liquid in penetration depth δ .

oscillation with a shear-horizontal polarization. Subsequently, any surface perturbation (within a penetration depth of 50 nm in aqueous solution) affects the amplitude and phase of the propagating wave; amplitude change (ΔA) is related to energy losses and viscoelastic phenomena, whereas phase change ($\Delta \Phi$) is related to mass deposition. The signal is measured with an HP 8753ES network analyzer, which was connected with an Agilent 3499A switch control unit in order to probe both sensors simultaneously.

2.2. Microfluidic module

Design issues: In order to select the optimum design for the microfluidic module, functionality issues and compatibility with the SAW chip had to be taken into consideration. More particularly, due to the piezoelectric nature of the sensor, the contact area with the separating walls of the module should be minimal; on the other hand, these walls should be thick enough in order to prevent inter-channel leakage. Furthermore, the microchannel should be spanning both sensors simultaneously, but not exceed the total width of the sensor chip. Thus, the microchannels' width and length were designed to be 1.1 and 12.75 mm, respectively; their depth was 100 μm , as it is defined by the fabrication procedure, and the separating wall between the microchannels was 120 μm . With these dimensions, each microchannel sensing area is 1.76 mm² (as opposed to 7.44 mm² of the total sensing area). Finally, hollow areas were designed to be located right above the IDT sets, so that the latter are protected from direct contact with the "bulk" material of the micromodule, avoiding severe signal distortion. The design appears in black in Fig. 2a.

Fabrication process & integration: PDMS was chosen as structural material for the microfluidic module, because it is an easy-to-process material, it conforms well on surfaces and thus seals well, and it presents no swelling when used with the described liquid samples. The fabrication procedure was soft lithography of PDMS

[11]. The AutoCAD design was printed on a transparency, which was used to prepare the mask. The latter was used for the structuring of a mold made of the epoxy resin SU8 (100 μm thick, which defines the depth of the microchannels) using negative lithography. Subsequently, PDMS was poured on the mold and after thermal treatment it was ready for use. After peeling off and dicing, vias with 500 μm diameter were drilled for capillary tubes attachment (Fig. 2b).

Concerning the adjustment of the module on the sensor chip, it was necessary to ensure the reusability of both the PDMS module and the sensor chip. Therefore, no plasma treatment was used since it causes permanent PDMS bonding. Instead, the attachment between the two parts was conducted by slightly pressing the module against the chip.

3. Evaluation of $\mu\text{F-on-SAW}$ with glycerol and protein solutions

A very important issue for the successful function of the $\mu\text{F-on-SAW}$ is to have a uniform sensitivity profile along the path of the acoustic wave. Once this is verified, the injection of multiple, different analytes will result in different signal responses due to sample differences, rather than sensitivity divergence between the sub-areas.

In order to test this, the same samples were injected into all microchannels. In particular, six aqueous glycerol solutions from 15% to 45% (w/w) were used. Such solutions do not adsorb on the sensor's surface and are removed completely upon water rinsing [4]. They are characterized by a particular density ρ and viscosity η , and the acoustic signal (either amplitude or phase) is proportional to the square root of density-viscosity product for the Newtonian region (where the six tested samples belong) [12,13].

The six samples were serially injected in microchannels 1–4 (with water rinsing in between each sample) using a syringe pump at a flow rate of 5 $\mu\text{L}/\text{min}$. The signal was monitored in real time and on both devices simultaneously. Fig. 3a shows the real time signal from device A. The equivalent graph for device B is similar to Fig. 3a (data not shown). One of the samples (32.8% w/w, indicated with arrows in Fig. 3a) was selected and its corresponding ΔA values from both devices appear in Fig. 3b, in a 2D array format. Each box corresponds to one of the eight formed sub-areas. As it appears, there is a remarkable uniformity and reproducibility in the signal response among the sub-areas of the same device (A1 vs. A2, B1 vs. B2, etc.) but also between equivalent sub-areas of different devices (A1 vs. B1, A2 vs. B2, etc.). The sensitivity S_i for each sub-area i appearing in Fig. 3a is extracted from the slope of

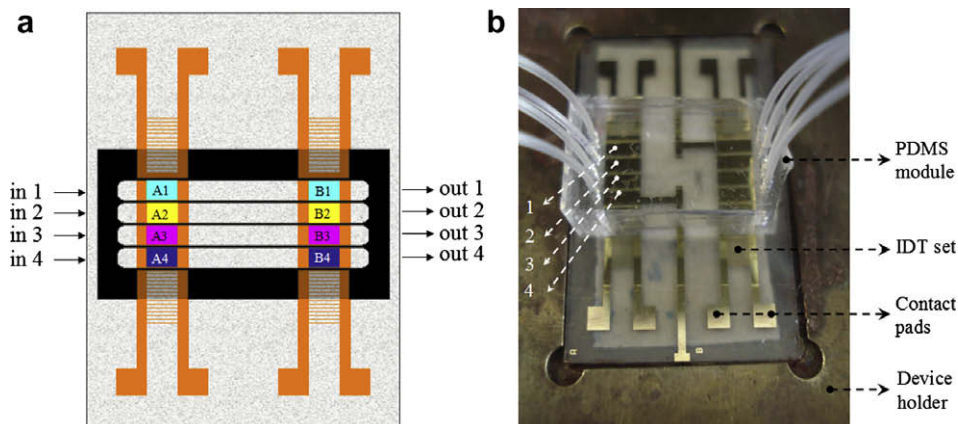


Fig. 2. (a) Schematic top view of the design as it is predicted to cross the devices, forming eight distinct sub-areas (A1, A2, ..., B3, B4); the arrows indicate the input and output of the samples. (b) Photo of the PDMS module mounted on the dual-sensor chip. # 1–4 denotes the microchannels.

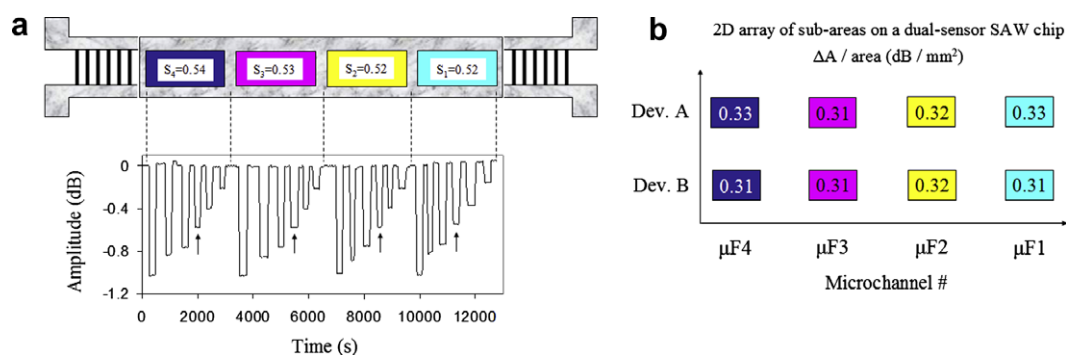


Fig. 3. (a) Real time change in wave amplitude at all sub-areas for the six glycerol solutions. S_1 – S_4 represent the sub-areas' sensitivity, expressed in $(\text{dB m}^2 \text{ s}^{1/2})/(\text{mm}^2 \text{ kg})$. (b) Surface-normalized ΔA for a particular glycerol sample (32.8% w/w) at each of the eight sub-areas formed on the dual SAW chip. The sub-areas' colors match those in Fig. 2a.

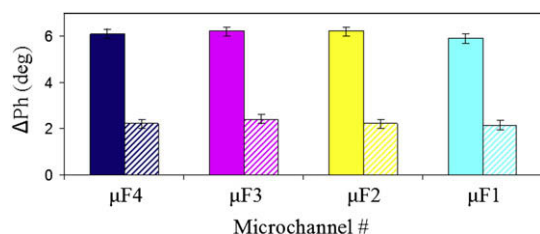


Fig. 4. Phase change for neu adsorption (solid bars) and subsequent b-BSA binding (striped bars) at the four sub-areas of one of the two sensors.

a ΔA vs. $\Delta(\rho\eta)^{1/2}$ graph (data not shown) deriving from all six samples used and proves to be very stable as well along the acoustic path.

Having proved the successful and reproducible detection of simple and non-adsorbing liquid samples with the μF -on-SAW, the setup was tested for biosensing implementation with protein solutions. Specifically, two protein solutions were used and two types of interactions were monitored: (i) physical adsorption of neutravidin (neu) in concentration 200 $\mu\text{g}/\text{ml}$ on the Au surface of the sensor, and (ii) subsequent specific binding of 200 $\mu\text{g}/\text{ml}$ biotinylated BSA (b-BSA). PBS buffer was used in the protein solutions and for the rinsing between the injections.

For protein samples, the phase of the acoustic wave was utilized instead of the amplitude, since the former is more sensitive to protein adsorption and/or binding; the signal changes are summarized in Fig. 4 for both proteins in one of the two sensors of the chip. It is evident that the process of neu adsorption is sensed very reproducibly among the four microchannels. This is also the case for the b-BSA binding on neu. The sub-areas were used in a varying sequence (i.e. 1 \rightarrow 2 \rightarrow 3 \rightarrow 4, vice versa and mixed) without noticing any effect on the reproducibility of the response. In addition, it is proved that a process taking place on a sub-area is independent of the “history” of the sample loading, i.e. the type of bound species and their location on the device, ensuring that

each microchannel compartment can host independent and non-interfering experiments.

4. Conclusions

A novel setup of microfluidics-on-SAW was described and evaluated in terms of sensitivity and signal response via aqueous glycerol solutions and protein adsorption and binding. It was proven that the reproducibility of the sensitivity among sub-areas of the array was as high as 92%, allowing multiple experiments to be carried out. This setup has potentials to extend its use to even larger number of analytes for (bio)medical applications.

Acknowledgements

K. Mitsakakis wishes to acknowledge Public Welfare Foundation “Propondis” for financial support. He also thanks A. Malainou and M.E. Vlachopoulou of IMEL, NCSR “Demokritos” for assistance in clean room processes and soft lithography, and Dr. F. Bender and Dr. A. Tsortos at I.M.B.B.-FO.R.T.H. for fruitful discussions.

References

- [1] G. Sauerbrey, Zeitschrift Phys. 155 (1959) 206.
- [2] K.K. Kanazawa, J.G. Gordon, Anal. Chim. Acta 175 (1985) 99.
- [3] S.J. Martin, G.C. Frye, Appl. Phys. Lett. 57 (1990) 1867.
- [4] K. Saha, F. Bender, A. Rasmussen, E. Gizeli, Langmuir 19 (2003) 1304.
- [5] A. Tsortos, G. Papadakis, K. Mitsakakis, K.A. Melzak, E. Gizeli, Biophys. J. 94 (2008) 2706.
- [6] A. Tsortos, G. Papadakis, E. Gizeli, Bios. Bioelectron. 24 (2008) 836.
- [7] M. Perpeet, S. Glass, T. Gronewold, A. Kiwitz, A. Malavé, I. Stoyanov, M. Tewes, E. Quandt, Anal. Lett. 39 (2006) 1747.
- [8] K. Länge, G. Blaess, A. Voigt, R. Götzen, M. Rapp, Biosens. Bioelectron. 22 (2006) 227.
- [9] K. Mitsakakis, A. Tserepi, E. Gizeli, JMEMS 17 (2008) 1010.
- [10] E. Gizeli, Anal. Chem. 72 (2000) 5967.
- [11] S.K. Sia, G.M. Whitesides, Electrophoresis 24 (2003) 3563.
- [12] A.J. Ricco, S.J. Martin, Appl. Phys. Lett. 50 (1987) 1474.
- [13] F. Josse, Z. Shana, J. Acoust. Soc. Am. 85 (1989) 1556.